Langmuir
Article
pubs.acs.org/Langmuir

Self-Assembly Mechanism for a Naphthalene−Dipeptide Leading to Hydrogelation

Lin Chen,[†] Kyle Morris,[‡] Andrea Laybourn,[†] David Elias,[†] Matthew R. Hicks,[§] Alison Rodger,[§] Louise Serpell,[‡] and Dave J. Adams*,[†]

[†]*Department of Chemistry, University of Liverpool, Crown Street, Liverpool, L69 7ZD, U.K.,* [‡]*Department of Chemistry and Biochemistry, School of Life Sciences, University of Sussex, Falmer, BN19QG, U.K., and* [§]*Department of Chemistry, University of Warwick, Coventry, CV4 7AL, U.K.*

Received September 30, 2009. Revised Manuscript Received November 5, 2009

Suitably functionalized dipeptides have been shown to be effective hydrogelators. The design of the hydrogelators and the mechanism by which hydrogelation occurs are both currently not well understood. Here, we have utilized the hydrolysis of glucono-δ-lactone to gluconic acid as a means of adjusting the pH in a naphthalene−alanylvaline solution allowing the specific targeting of the final pH. In addition, this method allows the assembly process to be characterized. We show that assembly begins as charge is removed from the *C*-terminus of the dipeptide. The removal of charge allows lateral assembly of the molecules leading to $\pi-\pi$ stacking (shown by CD) and β-sheet formation (as shown by IR and X-ray fiber diffraction). This leads to the formation of fibrous structures. Electron microscopy reveals that thin fibers form initially, with low persistence length. Lateral association then occurs to give bundles of fibers with higher persistence length. This results in the initially weak hydrogel becoming stronger with time. The final mechanical properties of the hydrogels are very similar irrespective of the amount of GdL added; rather, the time taken to achieving the final gel is determined by the GdL concentration. However, differences are observed between the networks under strain, implying that the kinetics of assembly do impart different final materials' properties. Overall, this study provides detailed understanding of the assembly process that leads to hydrogelation.

Introduction

There is currently significant interest in the use of oligopeptides and oligopeptide−conjugates as hydrogelators.[1−3] Specific examples include β-sheet forming oligopeptides,[4−7] α-helix forming oligopeptides,[8] PEO−peptide conjugates,[9] and recently di- and tripeptides conjugated to large aromatic groups such as fluorenylmethoxycarbonyl (Fmoc)[10−16] or naphthalene.[17−19] Low molecular weight gelators (LMWG) such as these oligopeptides self-assemble in solution to form long fibers that trap the water, forming a gel.[20,21] As such, hydrogels prepared from LMWG differ from hydrogels prepared by the cross-linking of polymeric chains in that they are reversible since they are held together by noncovalent interactions. Another potential advantage is that LMWG often have stimuli-responsive reversible sol−gel transitions, for example by pH[10,11,22] or temperature cycles.[23] As a result, hydrogels prepared from LMWGs have been suggested as an attractive method for the preparation of novel materials for applications such as drug release[18] and tissue engineering.[8,11,12,24]

The majority of dipeptides conjugated to Fmoc or naphthalene groups form hydrogels at low pH (<4).[11,17] A rare example is Fmoc−diphenylalanine, which forms hydrogels at physiological pH.[25] Recently, it has been shown that this is due to dramatic pK_a shifts induced by the high hydrophobicity of the molecule, with the assembly being controlled by the charge on the dipeptide.[26] However, it is not yet understood whether these observations are general or highly specific to a single system. Additionally, it is

*Corresponding author. E-mail: d.j.adams@liverpool.ac.uk.

(1) Ulijn, R. V.; Smith, A. M. *Chem. Soc. Rev.* **2008**, *37*, 664–675.
(2) Xu, B. *Langmuir* **2009**, *25*, 8375–8377.
(3) Bhattacharya, S.; Maitra, U.; Mukhopadhyay, S.; Srivastova, A. In *Molecular Gels: Materials with Self-Assembled Fibrillar Networks*; Weiss, R. G., Terech, P., Eds.; Springer: New York, 2005.
(4) Saiani, A.; Mohammed, A.; Frielinghaus, H.; Collins, R.; Hodson, N.; Kielty, C. M.; Sherratt, M. J.; Miller, A. F. *Soft Matter* **2009**, *5*, 193–202.
(5) Branco, M. C.; Pochan, D. J.; Wagner, N. J.; Schneider, J. P. *Biomaterials* **2009**, *30*, 1339–1347.
(6) Hule, R. A.; Nagarkar, R. P.; Altunbas, A.; Ramay, H. R.; Branco, M. C.; Schneider, J. P.; Pochan, D. J. *Faraday Discuss.* **2008**, *139*, 251–264.
(7) Krysmann, M. J.; Castelletto, V.; Kelarakis, A.; Hamley, I. W.; Hule, R. A.; Pochan, D. J. *Biochemistry* **2008**, *47*, 4597–4605.
(8) Banwell, E. F.; Abelardo, E. S.; Adams, D. J.; Birchall, M. A.; Corrigan, A.; Donald, A. M.; Kirkland, M.; Serpell, L. C.; Butler, M. F.; Woolfson, D. N. *Nat. Mater.* **2009**, *8*, 596–600.
(9) Tzokova, N.; Fernyhouph, C. M.; Topham, P. D.; Sandon, N.; Adams, D. J.; Butler, M. F.; Armes, S. P.; Ryan, A. J. *Langmuir* **2009**, *25*, 2479–2485.
(10) Adams, D. J.; Butler, M. F.; Frith, W. F.; Kirkland, M.; Mullen, L.; Sanderson, P. *Soft Matter* **2009**, *5*, 1856–1862.
(11) Jayawarna, V.; Ali, M.; Jowitt, T. A.; Miller, A. E.; Saiani, A.; Gough, J. E.; Ulijn, R. V. *Adv. Mater.* **2006**, *18*, 611–614.
(12) Jayawarna, V.; Smith, A.; Gough, J. E.; Ulijn, R. V. *Biochem. Soc. Trans.* **2007**, *35*, 535–537.
(13) Williams, R. J.; Smith, A. M.; Collins, R.; Hodson, N.; Das, A. K.; Ulijn, R. V. *Nat. Nanotechnol.* **2009**, *4*, 19–24.
(14) Mahler, A.; Reches, M.; Rechter, M.; Cohen, S.; Gazit, E. *Adv. Mater.* **2006**, *18*, 1365–1370.
(15) Yang, Z. M.; Gu, H. W.; Fu, D. G.; Gao, P.; Lam, J. K.; Xu, B. *Adv. Mater.* **2004**, *16*, 1440–1444.
(16) Jayawarna, V.; Richardson, S. M.; Hirst, A. R.; Hodson, N. W.; Saiani, A.; Gough, J. E.; Ulijn, R. V. *Acta Biomaterialia* **2009**, *5*, 934–943.
(17) Yang, Z. M.; Liang, G. L.; Ma, M. L.; Gao, Y.; Xu, B. *J. Mater. Chem.* **2007**, *17*, 850–854.
(18) Liang, G. L.; Yang, Z. M.; Zhang, R. J.; Li, L. H.; Fan, Y. J.; Kuang, Y.; Gao, Y.; Wang, T.; Lu, W. W.; Xu, B. *Langmuir* **2009**, *25*, 8419–8422.
(19) Yang, Z. M.; Liang, G. L.; Xu, B. *Chem. Commun.* **2006**, 738–740.
(20) de Loos, M.; Feringa, B. L.; van Esch, J. H. *Eur. J. Org. Chem.* **2005**, 3615–3631.
(21) Estroff, L. A.; Hamilton, A. D. *Chem. Rev.* **2004**, *104*, 1201–1217.
(22) Xing, B. G.; Yu, C. W.; Chow, K. H.; Ho, P. L.; Fu, D. G.; Xu, B. *J. Am. Chem. Soc.* **2002**, *124*, 14846–14847.
(23) Vegners, R.; Sheshtakova, I.; Kalvinsh, I.; Ezzell, R. M.; Janmey, P. A. *J. Peptide Sci.* **1995**, *1*, 371–378.
(24) Zhou, M.; Smith, A. M.; Das, A. K.; Hodson, N. W.; Collins, R. F.; Ulijn, R. V.; Gough, J. E. *Biomaterials* **2009**, *30*, 2523–2530.
(25) Smith, A. M.; Williams, R. J.; Tang, C.; Coppo, P.; Collins, R. F.; Turner, M. L.; Saiani, A.; Ulijn, R. V. *Adv. Mater.* **2008**, *20*, 37–41.
(26) Tang, C.; Smith, A. M.; Collins, R. F.; Ulijn, R. V.; Saiani, A. *Langmuir* **2009**, *25*, 9447–9453.

clear that the kinetics of the pH adjustment process are key in governing the final materials' properties of the hydrogels formed. Values for the storage modulus (G') for hydrogels prepared from Fmoc−diphenylalanine vary from 1 to 10^4 Pa.[14,25,26] We are interested in understanding the link between the kinetics of assembly and a material's final properties (which are vital for any specific application).

We recently demonstrated that the assembly process of a range of Fmoc−dipeptides could be followed utilizing the hydrolysis of glucono-δ-lactone (GdL) to adjust the pH.[10] GdL hydrolyzes slowly in water,[27] forming gluconic acid and hence lowering the pH of a solution in a controlled manner. To our knowledge, there is not a comparable system that can be added to a pH-dependent process to provide a controlled adjustment of pH. Here, gelation is pH-dependent, and so our aim was to use this reaction to provide the required pH change uniformly across the solution. The slow GdL hydrolysis (as compared to fast dissolution) allows the gelation process to be followed with time. In addition, the final pH achieved can be targeted by adjusting the amount of GdL added. Hence, this method can be used to prepare gels quiescently in the absence of a shear or processing history that often dominates the outcome of the gelation process. As noted above, for many systems, the outcome of the pH change is history-dependent and therefore different even between samples that are nominally identical. Using this methodology, we report here on the assembly of a naphthalene−dipeptide, utilizing the adjustable kinetics of pH change to follow the assembly process. We show that the assembly process translates directly onto the mechanical properties of the hydrogel, allowing a detailed understanding of the hydrogelation process.

Experimental Section

Materials. All chemicals and solvents were purchased from Sigma-Aldrich and used as received. Millipore water (resistivity = 18.2 MΩ·cm) was used throughout.

Naphthalene−Dipeptide Synthesis. The peptide derivative was prepared from 6-bromo-2-naphthol as follows.

To a stirred solution of 6-bromo-2-naphthol (5.0 g, 22.4 mmol) and potassium carbonate (15.48 g, 5 equiv, 112 mmol) in acetone (130 mL) was added chloro-*tert*-butyl acetate (3.52 mL, 1.1 equiv, 24.64 mmol). The solution was heated to reflux overnight. After this time, chloroform (100 mL) was added, and the solution was washed with water (4 × 100 mL). The organic phase was dried with magnesium sulfate and the solvent removed *in vacuo*. The crude product was purified by flash column chromatography, eluting with 10% ethyl acetate in hexane, to give *tert*-butyl 2-(6-bromonaphthalen-2-yloxy)acetate as an off-white solid in a 79% yield. ^{1}H NMR ($CDCl_3$): 7.92 (d, ArH, 1H, $^3J_{HH}$ = 2.0 Hz), 7.67 (d, ArH, 1H, $^3J_{HH}$ = 9.0 Hz), 7.57 (d, ArH, 1H, $^3J_{HH}$ = 8.8 Hz), 7.50 (dd, ArH, 1H, $^3J_{HH}$ = 2.0 Hz), 7.24 (dd, ArH, 1H, $^3J_{HH}$ = 2.6 Hz), 7.02 (d, ArH, 1H, $^3J_{HH}$ = 2.6 Hz), 4.62 (s, OCH_2C=O, 2H), 1.50 ppm (s, OC(CH_3)$_3$, 9H). ^{13}C NMR ($CDCl_3$): 168.2, 156.5, 133.2, 130.8, 130.1 (d, J = 7.2 Hz), 129.2, 128.9, 120.1, 117.9, 107.5, 83.0, 66.2, 28.5, 28.3 ppm. MS (CI, NH_3) 354 ([M + NH_4]$^+$). Accurate mass calculated: 354.070 48. Found: 354.069 75. Analysis calculated for $C_{16}H_{17}O_3Br$: C, 56.99%; H, 5.08%. Found: C, 56.90%; H, 5.06%.

The *tert*-butyl protecting group was removed by dissolving *tert*-butyl 2-(6-bromonaphthalen-2-yloxy)acetate (8.0 g, 23.7 mmol) in chloroform (ca. 30 mL). Trifluoroacetic acid (11.08 mL, 6.1 equiv, 145 mmol) was added, and the solution was stirred for 24 h. Hexane (200 mL) was added, and the resulting white precipitate was collected. After washing with hexane, the resulting solid was dried *in vacuo* to give 2-(6-bromonaphthalen-2-yloxy)acetic acid in a 92% yield. ^{1}H NMR (d_6-DMSO): 8.13 (d, ArH, 1H, $^3J_{HH}$ = 1.5 Hz), 7.85 (d, ArH, 1H, $^3J_{HH}$ = 9.0 Hz), 7.78 (d, ArH, 1H, $^3J_{HH}$ = 8.8 Hz), 7.57 (dd, ArH, 1H, $^3J_{HH}$ = 2.2 Hz), 7.32 (d, ArH, 1H, $^3J_{HH}$ = 2.6 Hz), 7.26 (dd, ArH, 1H, $^3J_{HH}$ = 2.6 Hz), 4.81 (s, OCH_2, 2H), 3.39 ppm (s, OH). ^{13}C (d_6-DMSO): 170.6, 150.7, 134.9, 132.2, 128.7, 127.1, 126.2, 126.1, 124.3, 123.0, 122.5, 72.3, 59.9 ppm. MS (CI, NH_3) 298 ([M + NH_4]$^+$), Accurate mass calculated: 298.007 88. Found: 298.007 99. Analysis calculated for $C_{12}H_9O_3Br$: C, 51.27%; H, 3.23%. Found: C, 50.91%; H, 3.18%.

The C-ethyl-protected alanine was coupled to 2-(6-bromonaphthalen-2-yloxy)acetic acid using standard coupling methodologies.[28] To a stirred solution of 2-(6-bromonaphthalen-2-yloxy)acetic acid (1.00 g, 3.56 mmol) in chloroform (20 mL) was added *N*-methylmorpholine (0.40 mL, 3.60 mmol), and isobutyl chloroformate (0.49 mL, 3.60 mmol) at 0 °C. The solution was stirred at 0 °C for 5 min. A solution of alanine ethyl ester (0.35 g, 2.5 mmol) and *N*-methylmorpholine (0.40 mL, 3.60 mmol) in chloroform (20 mL) was added. The solution was allowed to warm to room temperature and stirring continued overnight. The solution was washed with distilled water (2 × 100 mL), hydrochloric acid (2 × 100 mL, 0.1 M), aqueous potassium carbonate solution (100 mL, 0.1 M), and distilled water again (4 × 100 mL) and dried over magnesium sulfate, and the solvent was removed *in vacuo*. The solid was then washed with petroleum ether (10 mL) and dried under vacuum for 48 h to give ethyl 2-(2(6-bromonaphthalen-2-yloxy)acetamido)propanoate in a 73% yield. ^{1}H NMR ($CDCl_3$): 7.94 (s, ArH, 1H), 7.70 (d, ArH, 1H, $^3J_{HH}$ = 8.8 Hz), 7.62 (d, ArH, 1H, $^3J_{HH}$ = 8.3 Hz), 7.53 (d, ArH, 1H, $^3J_{HH}$ = 8.3 Hz), 7.26 (m, ArH, 2H, $^3J_{HH}$ = 8.3 Hz), 7.12 (s, ArH, 1H), 4.71 (m, CH_3CHC=O, 1H), 4.62 (s, OCH_2C=O, 2H), 4.23 (m, OCH_2CH_3, 2H, $^3J_{HH}$ = 7.0 Hz), 1.49 (d, NHCH(CH_3), 3H, $^3J_{HH}$ = 6.6 Hz), 1.29 ppm (t, OCH_2CH_3, 3H, $^3J_{HH}$ = 7.0 Hz). ^{13}C NMR ($CDCl_3$): 172.9, 167.8, 155.7, 133.1, 130.9, 130.4, 130.1, 129.0, 119.7, 118.3, 108.0, 67.7, 62.1, 48.2, 18.9, 14.5 ppm. MS (ES+, CH_3OH) 402 ([M + Na]$^+$), Accurate mass calculated: 402.0317. Found: 402.0317. Analysis calculated for $C_{17}H_{18}NO_4Br$: C, 53.70%; H, 4.77%; N, 3.68%. Found: C, 54.04%; H, 4.78%; N, 3.66%.

To deprotect the *C*-terminus, lithium hydroxide (0.2 g) was added to a solution of ethyl 2-(2(6-bromonaphthalen-2-yloxy)acetamido)propanoate (0.5 g) in a THF:water solution (3:1 mixture, 25 mL), and the solution was stirred for 18 h. After this time, distilled water (ca. 100 mL) was added, and then hydrochloric acid (1.0 M) was added dropwise until the pH was lowered to pH 3. The resulting white precipitate was collected by filtration and washed well with water and petroleum ether before being dried *in vacuo* to give 2-(2-(6-bromonaphthalen-2-yloxy)acetamido)propanoic acid as a white powder in 89% yield. ^{1}H NMR (d_6-DMSO): 8.44 (d, ArH, 1H, $^3J_{HH}$ = 7.5 Hz) 8.13 (d, ArH, 1H, $^3J_{HH}$ = 1.6 Hz), 7.86 (d, ArH, 1H, $^3J_{HH}$ = 8.8 Hz), 7.75 (d, ArH, 1H, $^3J_{HH}$ = 8.8 Hz), 7.58 (dd, ArH, 1H, $^3J_{HH}$ = 1.9 Hz), 7.34 (m, NH, 1H), 7.31 (dd, ArH, 1H, $^3J_{HH}$ = 2.4 Hz), 4.65 (m, OCH_2-C=O, 2H), 4.30 (m, $(CH_3)CHC$=O, 1H), 3.42 (s, OH), 1.33 (d, (CH_3)CHC=O, 3H, $^3J_{HH}$ = 7.2 Hz) ppm. ^{13}C (d_6-DMSO): 174.3, 167.5, 156.4, 133.0, 130.3, 129.7 (d, J = 5.7 Hz), 129.3, 129.0, 120.2, 116.9, 107.8, 67.1, 47.8, 17.6 ppm. MS (ES+, CH_3OH) 374 ([M + Na]$^+$). Accurate mass calculated: 374.0005. Found: 374.0004. Analysis calculated for $C_{15}H_{14}NO_4Br$: C, 51.16%; H, 4.01%; N, 3.96%. Found C, 51.16%; H, 4.02%; N, 3.96%.

A similar procedure was followed for the addition of the second amino acid.

Ethyl 2-(2-(2-(6-bromonaphthalen-2-yloxy)acetamido)propanamido)-3-methylbutanoate was prepared as a white solid in a 91% yield. ^{1}H NMR ($CDCl_3$): 7.92 (d, ArH, 1H, $^3J_{HH}$ = 1.6 Hz), 7.68 (d, ArH, 1H, $^3J_{HH}$ = 9.8 Hz), 7.59 (d, ArH, 1H, $^3J_{HH}$ = 8.7 Hz), 7.51 (dd, ArH, 1H, $^3J_{HH}$ = 8.7 Hz, $^3J_{HH}$ = 2.0 Hz), 7.22

(27) Pocker, Y.; Green, E. *J. Am. Chem. Soc.* **1973**, *95*, 113–119.

(28) Adams, D. J.; Young, I. *J. Polym. Sci., Part A: Polym. Chem.* **2008**, *46*, 6082–6090.

(dd, ArH, 1H, $^3J_{HH}$ = 9.1 Hz, $^3J_{HH}$ = 2.7 Hz), 7.16 (bd, NH, 1H, $^3J_{HH}$ = 7.3 Hz), 7.12 (d, ArH, 1H, $^3J_{HH}$ = 2.5 Hz), 6.52 (bd, NH, 1H, $^3J_{HH}$ = 8.8 Hz), 4.64 (m, C*H*NH, 1H), 4.51 (d, OCH_2, 2H, $^3J_{HH}$ = 2.2 Hz), 4.48 (d, C*H*NH, 1H, $^3J_{HH}$ = 8.7 Hz, $^3J_{HH}$ = 4.8 Hz), 4.21 (q, CH_2CH_3, 2H, $^3J_{HH}$ = 7.1 Hz), 2.15 (m, C*H*-$(CH_3)_2$, 1H), 1.44 (d, CHCH_3, 3H, $^3J_{HH}$ = 6.7 Hz), 1.28 (t, CH_2CH_3, 3H, $^3J_{HH}$ = 7.1 Hz), 0.91 (d, CH(CH_3), 3H, $^3J_{HH}$ = 7.0 Hz), 0.89 ppm (d, CH(CH_3), 3H, $^3J_{HH}$ = 7.0 Hz). ^{13}C NMR ($CDCl_3$): 171.5, 171.4, 167.7, 155.4, 132.8, 130.7, 130.0, 129.7, 129.0, 128.0, 119.2, 117.9, 107.9, 67.4, 61.2, 57.4, 48.6, 31.1, 18.8, 18.2, 17.6, 14.1 ppm. MS (CI) 498/496 ($[M + NH_4]^+$). Analysis calculated for $C_{22}H_{27}N_2O_5Br$: C, 55.12%; H, 5.68%; N, 5.84%. Found C, 55.03%; H, 5.72%; N, 5.81%.

2-(2-(2-(6-Bromonaphthalen-2-yloxy)acetamido)propanamido)-3-methylbutanoic acid was collected as a white solid in a 88% yield. ^{1}H NMR (d_6-DMSO): 8.20 (bd, NH, 1H, $^3J_{HH}$ = 7.6 Hz), 8.12 (d, ArH, 1H, $^3J_{HH}$ = 1.6 Hz), 8.06 (bd, NH, 1H, $^3J_{HH}$ = 8.5 Hz), 7.86 (d, ArH, 1H, $^3J_{HH}$ = 8.9 Hz), 7.76 (d, ArH, 1H, $^3J_{HH}$ = 8.8 Hz), 7.58 (dd, ArH, 1H, $^3J_{HH}$ = 8.8 Hz, $^3J_{HH}$ = 2.1 Hz), 7.34 (d, ArH, 1H, $^3J_{HH}$ = 1.6 Hz), 7.30 (dd, ArH, 1H, $^3J_{HH}$ = 8.9 Hz, $^3J_{HH}$ = 2.1 Hz), 4.66 (d, OCH_2, 2H, $^3J_{HH}$ = 2.2 Hz), 4.53 (m, C*H*NH, 1H), 4.15 (dd, C*H*NH, 1H, $^3J_{HH}$ = 8.6 Hz,$^3J_{HH}$ = 5.9 Hz), 2.04 (m, C*H*$(CH_3)_2$, 1H), 1.28 (d, CHCH_3, 3H, $^3J_{HH}$ = 7.1 Hz), 0.85 ppm (d, CH(CH_3)$_2$, 6H, $^3J_{HH}$ = 6.6 Hz). ^{13}C NMR (d_6-DMSO): 172.8, 172.2, 166.9, 155.9, 132.6, 129.9, 129.3, 129.2, 128.9, 128.6 119.7, 116.5, 107.5, 66.8, 57.1, 47.6, 29.8, 19.0, 18.4, 17.9 ppm. MS (CI) 468/470 ($[M + NH_4]^+$). Analysis calculated for $C_{20}H_{23}N_2O_5Br$: C, 53.23%; H, 5.14%; N, 6.21%. Found C, 52.93%; H, 5.11%; N, 6.18%.

NMR. ^{1}H NMR spectra were recorded at 400.13 MHz using a Bruker Avance 400 NMR spectrometer. ^{13}C NMR spectra were recorded at 100.6 MHz.

Gelation Studies. The dipeptide derivative (25.0 mg) was suspended in deionized water (5.00 mL). An equimolar quantity of NaOH (0.1 M, aq) was added, and the solution was gently stirred for 30 min until a clear solution was formed. The pH of this solution was measured to be 10.7. To prepare hydrogels, solutions were added to measured quantities of glucono-δ-lactone (GdL) according to the requirements of final pH, and the samples were left to stand for 24 h.

pH Measurements and pK_a Determination. A FC200 pH probe (HANNA instruments) with a (6 mm × 10 mm) conical tip was employed for all the pH measurements. The stated accuracy of the pH measurements is ±0.1. The pH changes during the gelation process were recorded every 1 min for 24 h. All measurements were conducted at room temperature. The pK_a values of dipeptide derivative (0.5 wt %) solutions were determined by titration via the addition of aliquots of a 0.1 M HCl solution. pH values were also recorded every 2 s during the titration process. To prevent the formation of gel, the solutions were gently stirred, thus keeping the solution liquid during the whole "titration" process.

Circular Dichroism and Linear Dichroism. Measurements were performed at room temperature (21 °C) on a Jasco J-815 spectropolarimeter modified for linear dichroism (Jasco UK, Great Dunmow, UK). Spectra were measured between 350 and 180 nm with a data pitch of 0.2 nm. The bandwidth was set to 2 nm with a scanning speed of 100 nm min^{-1} and a response time of 1 s. Spectra were collected at 2 min intervals. For clarity, the circular dichroism (CD) and linear dichroism (LD) figures show spectra only every 10 min. The path length was 0.1 mm in a demountable Spectrosil quartz cuvette (Starna Optiglass, Hainault, UK). Note that the sample was placed directly adjacent to the photomultiplier tube in order to minimize loss of light due to scattering. All measurements were performed in duplicate.

Rheology. Initial tests for gelation were carried out by simple vial inversion.[29] Typically, 2 mL of solution (with added GdL) was placed in a sample tube (22 mm diameter, 60 mm high). After standing for 24 h, the sample tube was inverted, with gelation being shown by a lack of flow. Dynamic rheological experiments were performed on an Anton Paar Physica MCR101 rheometer. In the oscillatory shear measurements, a sandblasted parallel top plate with a 50 mm diameter and 1.0 mm gap distance was used. Gels for rheological experiments were prepared on the bottom plate of the rheometer by loading a 2.0 mL solution of the gelator immediately after GdL addition. At this point, the sample is still a free-flowing liquid. Hence, sample uniformity and reproducibility are high. Evaporation of water from the hydrogel was minimized by covering the sides of the plate with low-viscosity mineral oil. The measurements of the shear modulus (storage modulus G' and loss modulus G'') with gelation were made as a function of time at a frequency of 1.59 Hz (10 rad/s) and at a constant strain of 0.5% for a period of 2 h, followed by an amplitude sweep from 0.01% to 100% under a frequency of 10 rad/s. The strain amplitude measurements were performed within the linear viscoelastic region, where the storage modulus (G') and loss modulus (G'') are independent of the strain amplitude. All the experiments were conducted at 25 °C.

Fluorescence Spectroscopy. Fluorescence spectra were obtained on a PerkinElmer luminescence spectrometer LS55. Thioflavin T (ThT) (0.1 mL of a 0.5 μM solution in water) was added to a solution of the dipeptide derivative (2 mL of a 0.5 wt % solution at pH 10.7). This was added to the required amount of GdL and immediately loaded into a 1.0 cm path-length cuvette. Emission spectra were collected every 5 min in the first 3 h and then every 30 min for 21 h. The emission spectra were recorded between 460 and 600 nm by excitation at 455 nm. The maxima emission peaks were at 485 nm. The slit width for emission and excitation was 2.5 nm, and the scan rate was 100 nm/min.

FTIR. IR spectra were collected on Bruker FTIR at 2 cm^{-1} resolution by averaging over 64 scans. All hydrogels were prepared in D_2O using NaOD (0.1 M) to change the pD. The hydrogels were loaded onto a CaF_2 windows, and another CaF_2 window was placed on the top of the gels. Each spectrum was background subtracted. For all spectra, the region between 1500 and 1800 cm^{-1} was shown in the figures after the peak of 1645 cm^{-1} was normalized to unity. The peak intensities were obtained by fitting the spectra with PEAKFIT software using Gaussian functions. The fitting coefficients were all above 0.98.

Transmission Electron Microscopy. Samples for examination by TEM were prepared *in situ* on Formvar/carbon film coated 400-mesh copper grids (Agar scientific). The required amount of GdL was added to a solution of dipeptide derivative (0.5 wt % solution at pH 10.7), and immediately grids were placed inverted onto 10 μL droplets of the gelation solution. In a humid chamber at room temperature, material was allowed to adsorb onto the grids and removed at specific time points followed by 5 min of drying and two 1 min negative stains using 2% w/v uranyl acetate. Grids to represent time zero were prepared by allowing adsorption of material for 1 min followed by negative staining as described. Negatively stained grids were allowed to dry and examined on a Hitachi-7100 TEM operated at 100 kV. Images were acquired digitally using an axially mounted (2000 × 2000 pixels) Gatan Ultrascan 1000 CCD camera (Gatan, Oxford, UK).

X-ray Fiber Diffraction. Fiber diffraction samples were prepared *in situ* from dipeptide solutions with varying amounts of GdL for final pH targeting. By placing a 10 μL droplet between two wax filled capillary tubes and allowing the solution to gelate and air-dry, a partially aligned fiber sample was formed (as previously described[30]). The fiber sample was mounted on a goniometer head, and X-ray diffraction data were collected using a Rigaku Cu Kα (wavelength 1.5419 Å) rotating anode and RAxis IV++ detector with exposure times of 10−20 min and specimen-to-detector distances of 200 mm. The diffraction images were

(29) Raghavan, S. R.; Cipriano, B. H. In *Molecular Gels: Materials with Self-Assembled Fibrillar Networks*; Weiss, R. G., Terech, P., Eds.; Springer: New York, 2005.

(30) Makin, O. S.; Serpell, L. C. In *Amyloid Proteins: Methods and Protocols*; Sigurdsson, E. M., Ed.; Humana Press: Totowa, 2005; pp 67−80.

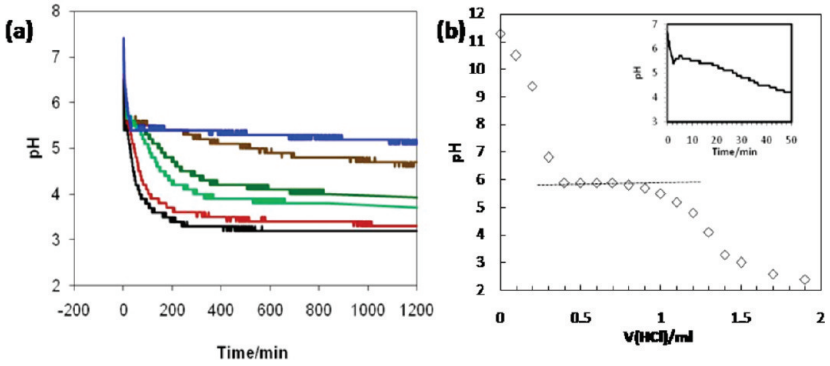

Figure 1. (a) Change in pH with time for aqueous solutions of dipeptide derivative (0.5 wt %) added to different amounts of GdL. In all cases, the initial pH was 10.7. Added GdL: (blue) 1.82 mg/mL, final pH = 5.1; (brown) 2.94 mg/mL, final pH = 4.7; (dark green) 4.46 mg/mL, final pH = 4.0; (light green) 5.96 mg/mL, final pH = 3.7; (red) 9.72 mg/mL, final pH = 3.3; (black) 14.42 mg/mL, final pH = 3.1. The final pH is quoted after 20 h. (b) Titration curve for the dipeptide solution with HCl (0.1 M) and pH changes curve in the first 50 min (inset) on adding dipeptide solution to GdL (14.42 mg/mL).

Scheme 1

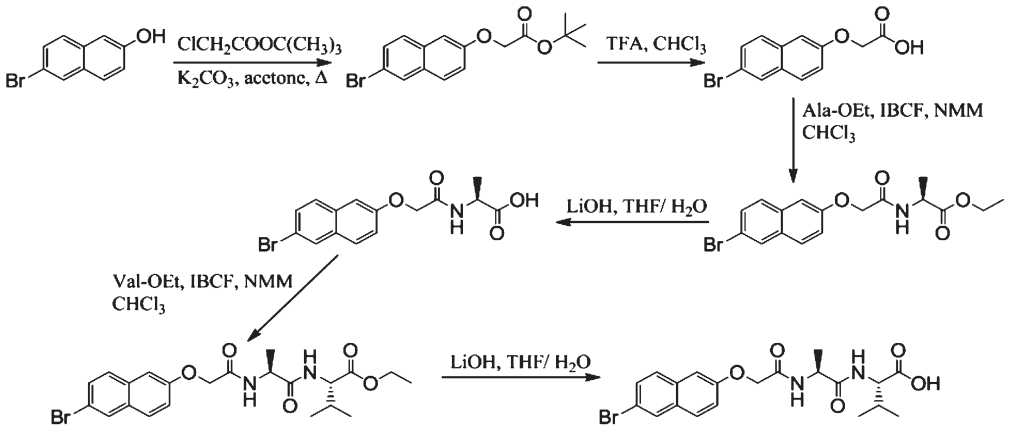

examined using CLEARER,[31] and the diffraction signal positions were determined using a module within CLEARER.

Results and Discussion

The dipeptide derivative was synthesized from the commercially available 6-bromo-2-naphthol as shown in Scheme 1. Using this methodology, the naphthalene−dipeptide was recovered in high yield and purity (>98%, as evidenced by both NMR and elemental analysis).

This peptide derivative is related to the naphthalene−dipeptides reported by Yang et al.,[17] although here the naphthalene ring is also substituted with a bromine atom. This provides extra hydrophobicity compared to the parent naphthalene−dipeptide, which is a poor gelator (data not shown). An aqueous solution of the dipeptide derivative at a concentration of 0.5 wt % was prepared by addition of an equimolar amount of sodium hydroxide to a suspension of the dipeptide conjugate in deionized water. The final pH after peptide dissolution was found to be 10.7. The dipeptide derivative was found to be stable in aqueous solution at high pH for extended periods of time. To induce assembly, the solution was added to a specific amount of GdL. The kinetics of the pH change and the final pH of the solution were found to correlate with the amount of GdL used. Figure 1a shows that the pH drops rapidly initially, before reaching a pH of ~5.4. Here, buffering occurs as the pK_a of the peptide derivative is reached. This value for the pK_a is higher than might be expected for the *C*-terminus of a peptide. However, it has recently been reported that the pK_a of the *C*-terminus of Fmoc-diphenylalanine is significantly higher than expected.[26] In line with this report, we carried out a "titration" of the dipeptide derivative with 0.1 M HCl solution. This confirmed that the pK_a of the dipeptide derivative was indeed higher than expected at around 5.9 (Figure 1b). Only a single pK_a was observed. With GdL, buffering occurs at a slightly lower pH of 5.4. It is also common to see a slight increase in pH after the initial buffering (the inset picture of Figure 1b). We ascribe this to the pK_a of the initial kinetic aggregates being higher than that of the dipeptide. Hence, on aggregation, if a relatively rapid change of the aggregates from carboxylate terminated to carboxylic acid terminated is quicker than the hydrolysis of GdL can provide further protons, an apparent pH increase will occur. The pH then continues to drop over time before reaching equilibrium.

For systems where the pH is below 5.0, self-supporting hydrogels were formed (as determined by simple vial inversion). The secondary structure of peptides (including dipeptides on gelation) has been probed previously by IR.[7,9,26,32] We measured the IR of gels prepared at a range of concentrations of GdL. The data in Figure 2a show that at high pH weak peaks at 1628 and 1679 cm^{-1} (normally ascribed to the presence of antiparallel β-sheets[32]) are observed. A stronger peak at 1645 cm^{-1}, which could be indicative of a random coil structure,[32] was observed. An

(31) Makin, O. S.; Sikorski, P.; Serpell, L. C. *J. Appl. Crystallogr.* **2007**, *40*, 966–972.

(32) Pelton, J. T.; McLean, L. R. *Anal. Biochem.* **2000**, *277*, 167–176.

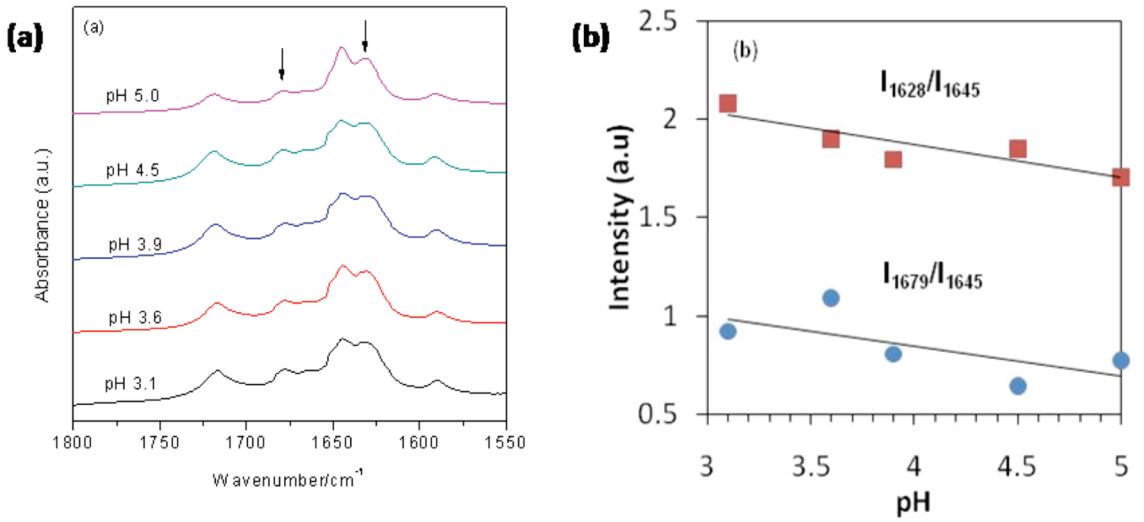

Figure 2. (a) IR spectra collected after 20 h from hydrogels prepared at a number of different pH. (b) Ratio of intensity of the peaks at 1629 and 1679 cm^{-1} relative to that at 1645 cm^{-1} increase as the pH decreases. The lines have been added as a guide to the eye.

alternative explanation for this peak is from the stretching of −C═C− in the naphthalene ring. At lower pH, the signals ascribed to the presence of β-sheet become stronger as compared to that at 1645 cm^{-1} (Figure 2b). As expected considering the pK_a of the dipeptide derivative, there is a peak at 1718 cm^{-1} present across the pH range measured, ascribed to the terminal COOH of the dipeptide. Recent data for Fmoc-diphenylalanine showed only the presence of two peaks, one at 1630 cm^{-1} and a second at 1685 cm^{-1}, both of similar intensity.[25,26] No peak at 1718 cm^{-1} was observed, implying that the terminal carboxylic acid is not protonated. These data were ascribed to the presence of antiparallel β-sheets. However, it is clear that the data reported for Fmoc-diphenylalanine, while similar to that reported here, are subtly different. This may indicate a slightly different packing arrangement of the dipeptide derivatives on assembly.

To probe further the interactions between the dipeptide molecules as the pH decreases, absorbance, CD, and LD spectra were recorded as a function time (which means as a function of pH in these experiments) following the addition of GdL to the solution to give a final GdL concentration of 14.42 mg/mL. The absorbance spectrum recorded for the dipeptide derivative at high pH has a very small signal above 300 nm, a medium strength signal at from 250 to 290 nm, and an intense band from 210 to 240 nm. Fine structure can be observed between 260 and 290 nm on careful inspection (Figure 3b). This structure is similar to that seen for naphthalene and substituted naphthalene compounds.[33] Thus, we can ascribe the 260−280 nm region to a naphthalene $\pi-\pi^*$ short axis polarized transition.[34] Similarly, much of the 230 nm intensity can be ascribed to an intense long axis polarized $\pi-\pi^*$ transition of the naphthalene. The peptide transitions are much weaker than those of naphthalene as shown by the decrease in absorbance between 200 and 220 nm, which is where the peptide bands have increasing intensity. Previously reported data for naphthalene−dipeptide conjugates showed a Cotton effect at 240 nm and a peak at 288 nm, ascribed to the $\pi-\pi^*$ transition of the naphthalene.[17]

Figure 3a shows the CD spectra of the naphthalene−peptide conjugates as a function of time (and hence pH). Naphthalene by itself is achiral and has no CD signal. In accord with this, the high-pH spectra show little or no CD signal when the conjugate is free in solution. However, as the pH drops, intense CD signals become increasingly apparent, indicating that the molecules are assembling into a chiral structure. The final CD magnitude (occurring at 60 min where the pH is measured to be 4.0 from Figure 1a, with no change thereafter) is high, indicating a highly asymmetric structure. The 260−280 nm short axis polarized naphthalene region gives a broad negative CD band with structure analogous to that observed in the absorbance spectra (Figure 3b, inset). At lower wavelength, the appearance of the spectrum is that of an overlay of exciton bands from 250 nm down. An exciton signal in a CD spectrum results from the coupling of degenerate transitions on nearby chromophores. The characteristic features of an isolated exciton band is that there are neighboring positive and negative bands with a fairly sharp transition between them whose zero point is at the maximum of the absorbance signal. When exciton bands overlay due to multiple transitions the picture becomes more complicated. In this case, the first exciton band is apparent as a large negative band at 236 nm and a positive component (apparent as a less negative minimum in Figure 3a) at 218 nm. Thus, the 230 nm band observed in the absorbance spectrum has split into a high-energy component and a low-energy component as a result of a chiral arrangement of the naphthalene chromophores.[35] If the chirality arises by a structure where the naphthalene chromophores are stacked one on top of the other, the sign pattern of the exciton CD spectrum can be interpreted following the line of argument in ref 35. The sign pattern observed here means that the long axes of two naphthalene chromophores are oriented[35] so the angle between them is between 0° and 90°, and they form a left-handed helix. As an aside, we note that the CD spectrum remains the same even if the sample is rotated through 90° (Figure 3d), thus verifying that the above discussion does relate to the true CD not a spectrum dominated by LD artifacts.

Recent data for a hydrogel prepared from Fmoc-diphenylalanine showed the presence of a strong negative CD signal at 218 nm, ascribed to the formation of a β-sheet structure.[25] No evidence was observed here for such a negative peak; however, this may simply be because the naphthalene chromophores

(33) Perkampus, H. *UV-Vis Atlas of Organic Compounds*, 2nd ed.; VCH Weinheim: New York, 1992.
(34) Rajendra, J.; Baxendale, M.; Rap, L. G. D.; Rodger, A. *J. Am. Chem. Soc.* **2004**, *126*, 11182–11188.
(35) Rodger, A.; Norden, B. *Circular Dichroism and Linear Dichroism*, 1st ed.; Oxford University Press: New York, 1997.

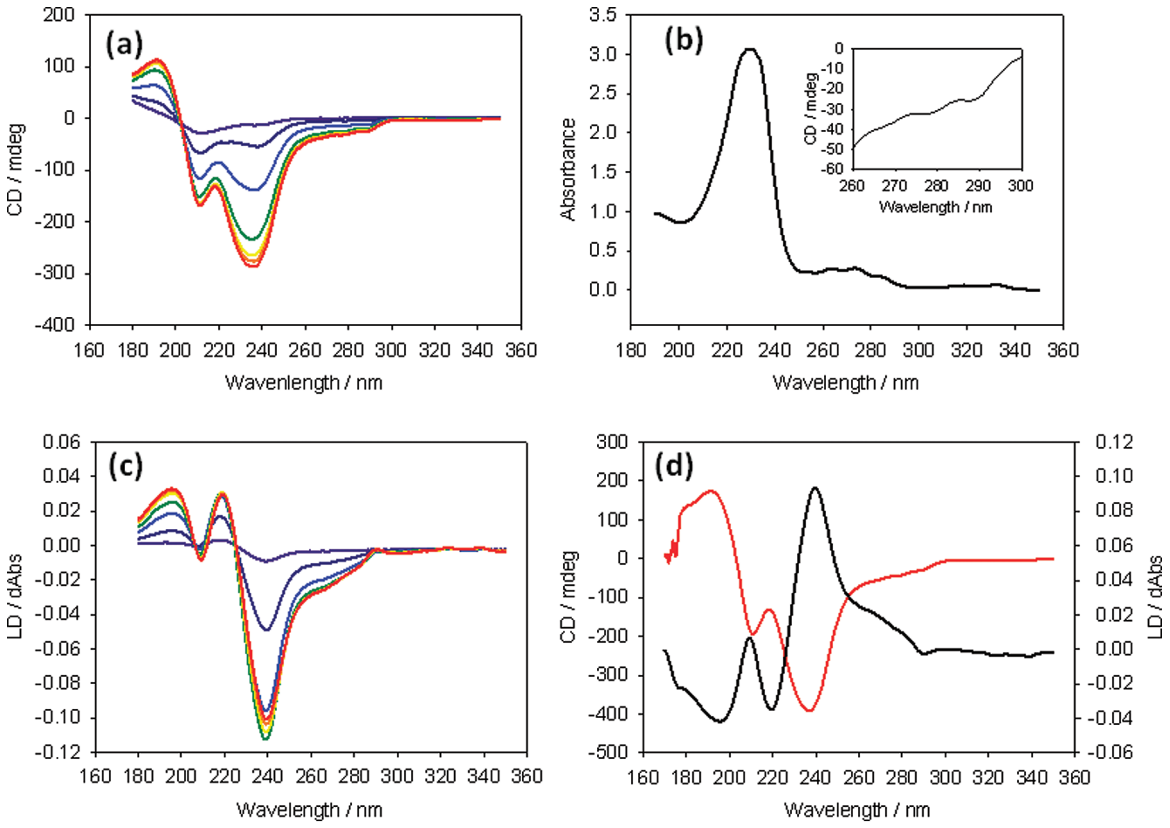

Figure 3. (a) Evolution of CD with time on addition of a solution of dipeptide derivative (0.5 wt %) to GdL (14.42 mg/mL). Data are shown for 0 min and then subsequently every 10 min. Signals increase with time. (b) UV−vis spectrum for dipeptide derivative at pH 10.7. Inset is an expansion of the CD after 1 h showing fine structure between 290 and 270 nm. (c) Evolution of LD with time on addition of a solution of dipeptide (0.5 wt %) to GdL (14.42 mg/mL). Data are shown for 0 min and then subsequently every 10 min. Signals increase with time until 50 min, when the magnitude decreases once again. (d) CD (red) and LD (black) spectra for sample formed 60 min after GdL addition with cell rotated through 90° (pH = 4.0 from Figure 1a).

dominated the observed spectrum due to their high extinction coefficient and consequent effective $\pi-\pi$ coupling.

The CD signal of $\pi-\pi$ systems is dominated by nearest-neighbor couplings. In order to try to determine how the naphthalene chromophores were oriented in the extended structure we assumed was present in the hydrogel, we measured the LD as a function of time (and hence pH) since it reports on the macroscopic anisotropy. LD is the difference in absorbance of light polarized parallel and perpendicular to an orientation axis. Samples were prepared in the cuvettes as before, with any alignment arising simply from structure formation in the cell. Here, the spectrum again changed over the first 40 min, with the magnitude of the signals increasing, before beginning to decrease again at 50 and 60 min (Figure 3c). The magnitude of the LD signals depended on the sample, with variation being observed between nominally identical samples (unlike the CD spectra which were of very similar intensity for different samples). As expected, the LD spectrum is inverted on rotating the sample through 90° (Figure 3d). From the CD band signs we know that the 236 nm signal results from the out-of-phase coupling (thus perpendicular to the line between the long axes of the napthalenes) of the transition moments[35] and the 218 nm signal from in-phase coupling. If the naphthalenes are stacked vertically like steps on a ladder, then both transitions would be expected to have a negative LD. This is in contrast to what is observed here. This means that the naphthalene long axes are tilted by more than 35° from the perpendicular. (LD = $3\cos^2\alpha - 1$, where α is the angle between the orientation axis and the transition moment. As LD = 0 for α = 54.7°, we deduce that the tilt must ensure the naphthalene's are tilted so they lie less than 54.7° from the orientation axis of the sample.)

To follow the assembly and gelation process, thioflavin T (ThT) was used as a fluorescent probe. ThT is widely used to probe the formation of β-sheet structures, especially in amyloid-forming peptides.[36,37] Recent results suggest that ThT acts as a molecular rotor.[38] Molecular rotors are viscosity-sensitive molecules, with a well-defined relationship between viscosity and fluorescence quantum yield.[39] Hence, an increase in local viscosity results in a significant increase in observed fluorescence. Liang et al. have demonstrated that Congo Red, a stain for amyloidogenic peptides, can also be used to stain fibers prepared from naphthalene−di- or tripeptides.[40] Since the IR data above demonstrate the presence of β-sheet structures, we rationalized that ThT could be used to probe the local structure as gelation occurred. ThT was therefore directly incorporated in the stock solution of the dipeptide derivative at pH 10.7. The lack of change in fluorescence at early time points indicates that assembly only begins when the pH reaches the pK_a of the dipeptide derivative (Figure 4): no increase in fluorescence is observed until a pH of 5.4

(36) Hawe, A.; Sutter, M.; Jiskoot, W. *Pharm. Res.* **2008**, *25*, 1487–1499.
(37) Lindgren, M.; Sorgjerd, K.; Hammarstrom, P. *Biophys. J.* **2005**, *88*, 4200–4212.
(38) Stsiapura, V. I.; Maskevich, A. A.; Kuzmitsky, V. A.; Uversky, V. N.; Kuznetsova, I. M.; Turoverov, K. K. *J. Phys. Chem. B* **2008**, *112*, 15893–15902.
(39) Haidekker, M. A.; Theodorakis, E. A. *Org. Biomol. Chem.* **2007**, *5*, 1669–1678.
(40) Liang, G. L.; Xu, K. M.; Li, L. H.; Wang, L.; Kuang, Y.; Yang, Z. M.; Xu, B. *Chem. Commun.* **2007**, 4096–4098.

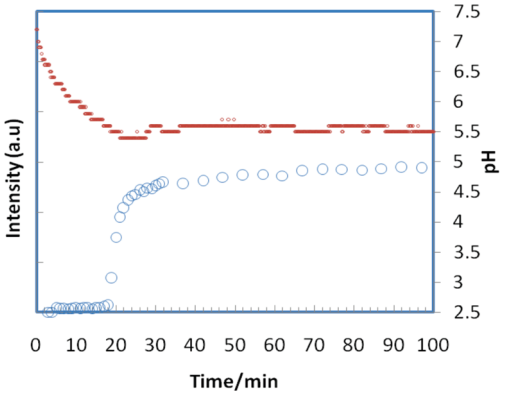

Figure 4. Change in ThT fluorescence at 485 nm (λ_{ex} = 455 nm) on addition of a solution of dipeptide derivative (0.5 wt %) to GdL (2.94 mg/mL) (blue data). Overlaid is the change of pH with time (red data from Figure 1).

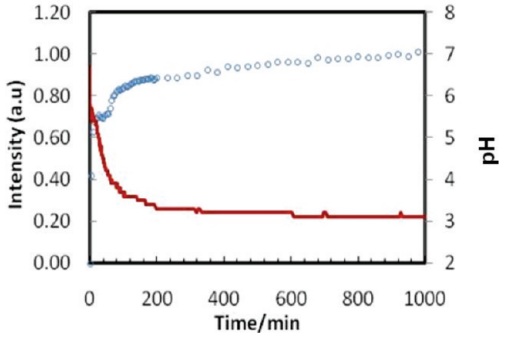

Figure 5. Normalized change in ThT fluorescence at 485 nm (λ_{ex} = 455 nm) on addition of solutions of dipeptide derivative to GdL (blue data). Overlaid is the change in pH with time (red data). The initial pH was 10.7. Amount of GdL added 14.42 mg/mL; final pH = 3.1.

is reached, following which a rapid increase in fluorescence is observed.

The change in ThT fluorescence over a longer time resulting from the addition of GdL to a solution of the dipeptide derivative is shown in Figure 5. From these data, it can be seen that there is a rise to a plateau (that observed in Figure 4), followed by a second rise to a plateau. This behavior is exhibited at a number of GdL concentrations (see Supporting Information).

Interestingly, the initial increase in fluorescence to the first plateau occurs while the systems are still liquid (see below for rheology data in Figure 9). This is in agreement with data obtained previously for Fmoc−leucine−glycine,[10] where fibers were imaged at early times before gelation occurred. The data obtained here indicate that assembly occurs by a two-stage process. Further analysis demonstrates that while the time at which the first plateau is reached is determined by the amount of GdL added (and hence the kinetics of pH change), the absolute pH at which this transition occurs is extremely similar in each case at pH 5.2 (see Supporting Information). This indicates that this transition is dependent on the pH of the solution, rather than the time taken to reach this pH. The end of the plateau occurs at different pH values depending on the amount of GdL added but occurs more quickly at higher quantities of GdL.

Using this information, the system was further probed by transmission electron microscopy (TEM). A solution containing 14.42 mg/mL of GdL was prepared. Aliquots were removed and allowed to gel for defined times. At these times, the samples were analyzed by TEM. The time course in Figure 6 shows that immediately after the addition of GdL ill-defined structures are formed. After 40 min (pH 4.2 from Figure 1a), some fibers with a minimum width of 12.9 nm (SD ± 0.97 nm, n = 10) were observed. After 80 min (pH 3.8), a large number of fibers were imaged. There is clear evidence for lateral association between fibers. Thicker structures are formed via the association of thinner fibers with a width of 12.0 nm (SD ± 0.50, n = 10) (Figure 7). The associated fibers have a higher persistence length than the thinner fibers. The micrographs taken at later times appear very similar showing a network of fibers, the majority of which are thicker than the original fibers formed at earlier time points. In contrast to results previously reported for naphthalene−dipeptides,[17] no helical structures were observed.

TEM was also used to probe the structures formed after 24 h in the systems with different amounts of added GdL. Here, the role of the final pH of the sample was examined. As can be seen from Figure 8, at a final pH of 5.0, the fibers formed are narrow with a minimum width of 10.5 nm (SD ± 1.53, n = 10); these fibers are comparable to the thinnest fibers observed at early time points (Figure 6). These fibers are likely to represent a basic protofilament. At pH 4.5 and below, similar structures were imaged but some of them with larger widths, in one instance measuring 25.4 nm (SD ± 1.83, n = 10). These also look very similar to the final structures prepared during the time course experiment (Figure 6) and are indicative of laterally associated protofilaments.

From the collective data shown above, it is clear that the self-assembly of the dipeptide derivative occurs via $\pi-\pi$ stacking and hydrogen bonding as would be expected. β-Sheet formation occurs, with the apparent degree of β-sheet increasing at lower pH. We have shown how GdL can be used to control the pH of the solution in a uniform fashion. The concentration of GdL added determines the final pH, and time determines how far along the route to the final pH that the solution is. The kinetics of assembly are determined by the rate of pH change in these experiments. In addition, the nature of the final hydrogel formed is dependent on the final pH of the solution, which we can also control by adding the appropriate amount of GdL to the starting mixtures. From these data, it is apparent that the kinetics of hydrogel formation and final material properties of the hydrogels would be expected to correlate with the amount of GdL added since this determines pH. Control of the material properties is key for final applications. The mechanical properties of the hydrogels prepared using different amounts of GdL were therefore probed by rheology. As reported previously for Fmoc−dipeptides and amino acids with GdL,[10] the development of the gel structure with time was probed *in situ*. Figure 9 shows the time evolution of storage modulus (G') and loss modulus (G'') with time for the gelation process of the dipeptide derivative using different amounts of GdL. In all cases, the gel strength (as measured by the storage modulus, G') increases with time before coming to a plateau value. Initially, the storage modulus and the loss modulus are similar in value as expected for a liquid. With time, G' dominates over G'' as expected for a true hydrogel. It should be noted that the gelation point (i.e., where $G' = G''$) occurred at a very early stage (less than 30 min). The kinetics of the development of the gel network depends on the amount of GdL, correlating well with the kinetics of the pH change. However, the final plateau values for both G' and G'' are extremely similar. The exception is for the lowest concentration of GdL, where a slightly lower value was obtained. However, the values for the modulii after 48 h were very similar to those shown for the higher GdL concentrations (data not shown). These data indicate

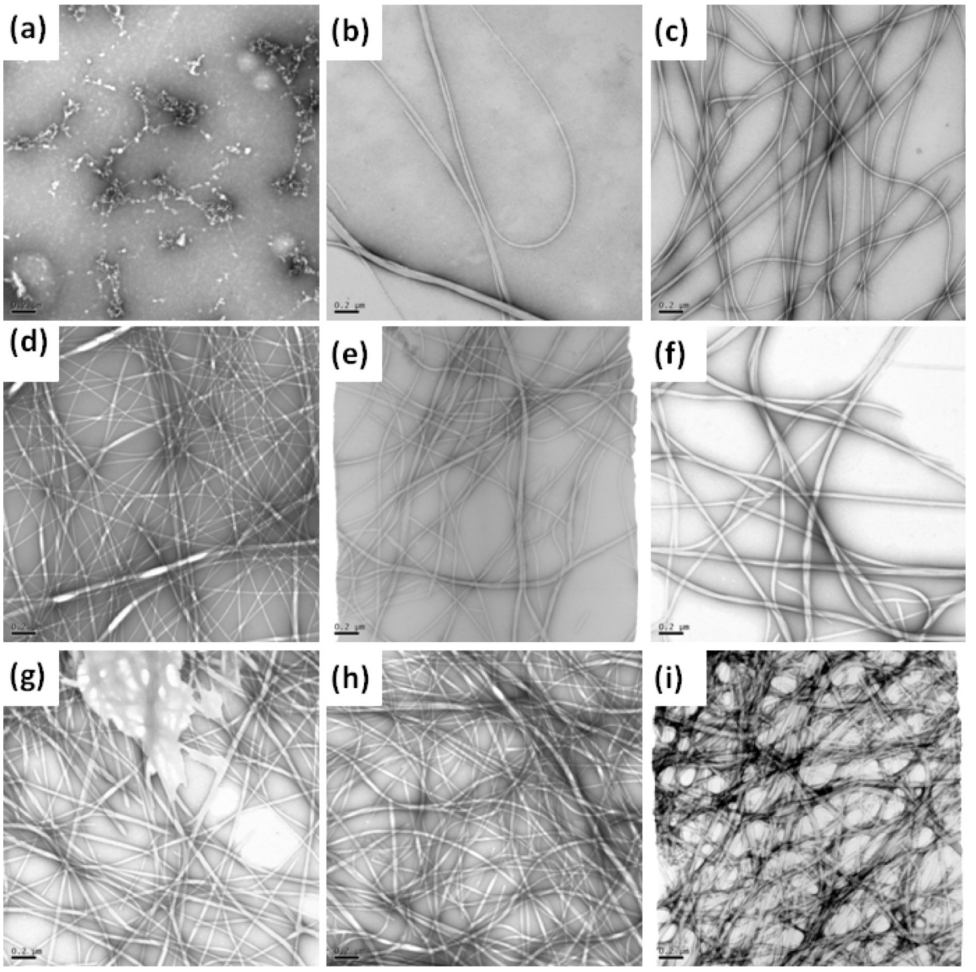

Figure 6. TEM of evolution of structures with time for dipeptide in the presence of GdL (14.42 mg/mL): (a) immediately after GdL addition; (b) 40 min, (c) 80 min, (d) 120 min, (e) 160 min, (f) 200 min, (g) 240 min, (h) 280 min, and (i) 400 min after GdL addition. In all cases, the scale bar represents 200 nm.

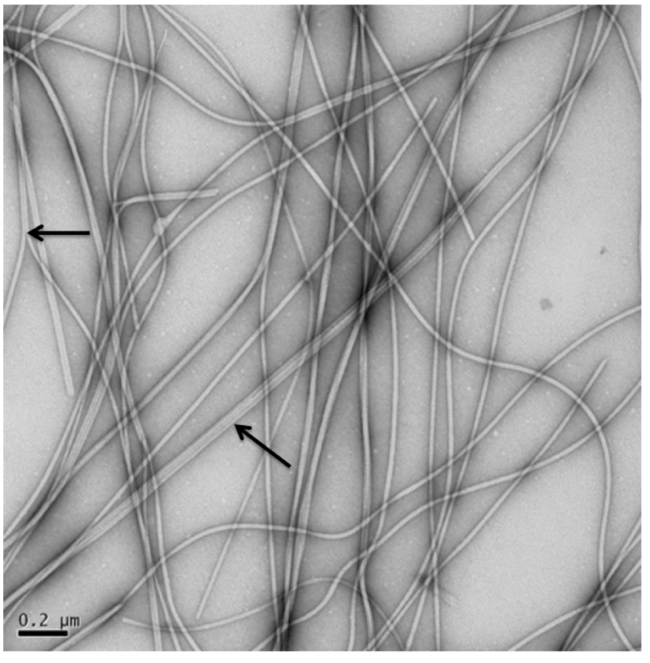

Figure 7. TEM of fibers formed 80 min after GdL addition. Associated fibers are highlighted with a black arrow. The scale bar represents 200 nm.

that the three-dimensional network structures that contribute to the mechanical properties are very similar in all cases after 24 h, despite the different kinetic pathway by which these networks are formed. We also note that the final value for the storage modulus (G') of ~57 000 Pa is significantly greater than that previously reported for a naphthalene−dipeptide (~8000 Pa).[17] We ascribe this to either the use of GdL to change the pH uniformly across the reaction mixture, thus achieving a uniform hydrogel, since a similar effect was noted for Fmoc−dipeptide systems,[10] or the higher hydrophobicity of the dipeptide derivative used here.

Among all material viscoelasic functions, complex viscosity (η^*) is considered as another sensitive parameter to structural changes during gelation.[41] Figure 10 shows the time dependence of η^* overlaid with the intensities of emission peaks of ThT during the gelation process for systems using different concentrations of GdL. This data demonstrate that the evolution of structure as demonstrated by rheological measurements correlates well with the fluorescence data. In all cases, a two-stage process occurs, with the kinetic profile being dependent on the amount of GdL added. Similar to the behavior of intensities of ThT emission peaks with time, η^* increased with the gelation. They also show two-stage evolutions.

Despite similarities in G' and G'' between different systems, the impact of the kinetics of gel formation can be observed in the

(41) Weng, L. H.; Chen, X. M.; Chen, W. L. *Biomacromolecules* **2007**, *8*, 1109–1115.

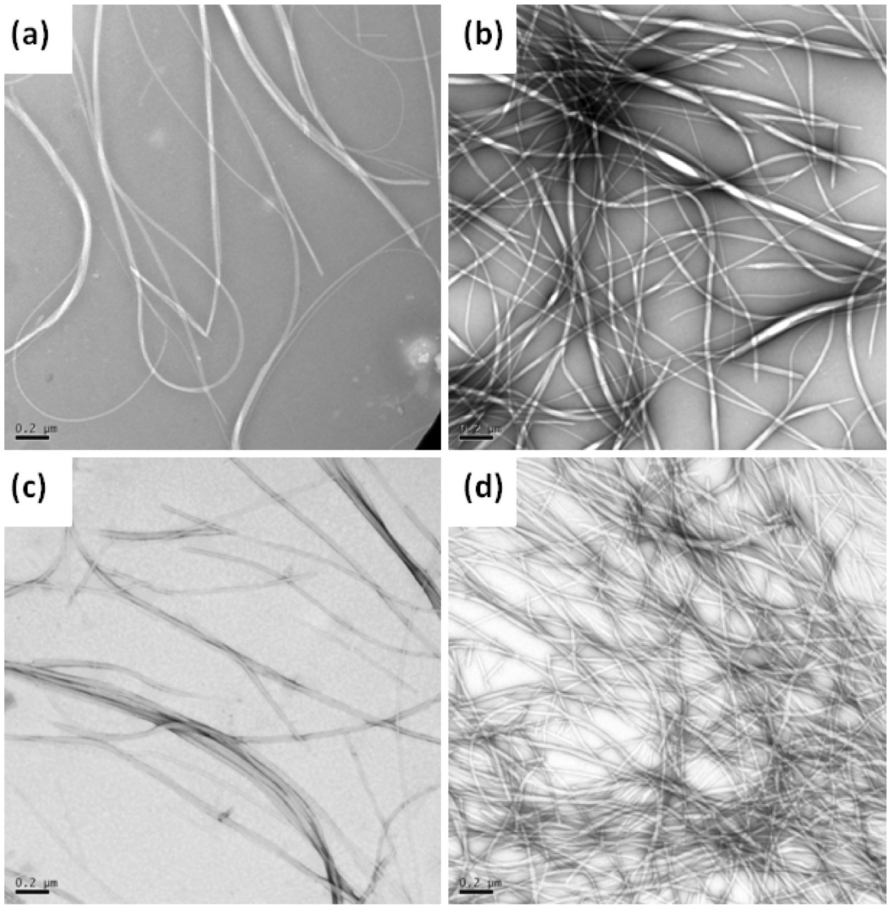

Figure 8. TEM of fibers formed after 24 h in dipeptide hydrogels (0.5 wt %) with different amounts of added GdL: (a) 1.82 mg/mL, final pH = 5.0; (b) 2.94 mg/mL, final pH = 4.5; (c) 5.96 mg/mL, final pH = 3.6; (d) 14.42 mg/mL, final pH = 3.1. The scale bar in each case represents 200 nm.

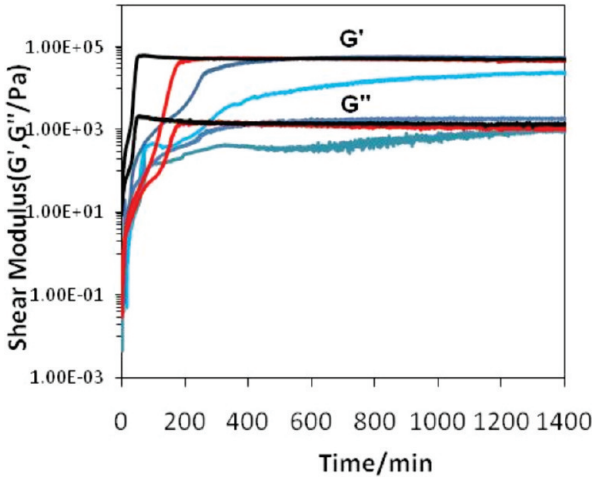

Figure 9. Evolution of G' and G'' with time for solutions of the dipeptide (0.5 wt %) with different amounts of GdL. Concentrations of GdL used: (black) 14.42 mg/mL, (red) 5.96 mg/mL, (dark blue) 4.46 mg/mL, and (light blue) 2.94 mg/mL.

amplitude sweeps for the hydrogels shown in Figure 11. Here, the hydrogel prepared using 14.42 mg/mL GdL (i.e., final pH 3.1) was found to be the most stable under external force, with the transition from "gel-like" to "liquid-like" (as demonstrated by the crossover point where G' is no longer greater than G'') is around 5%. At which, there is a rapid decline of G', indicating the breakdown of hydrogel structures. This is similar to that reported elsewhere for gels prepared using di(*p*-toluoyl)-L-cystine.[42] The gels formed with less GdL at a higher final pH (pH = 4.0 and 4.5) are less tolerant to strain, with the turning points occurring at ~1%. However, the crossover point from "gel-like" to "liquid-like" occurs at much higher strain in these systems at approximately 8−10%. This failure behavior implies that the fibrils forming the matrix of the hydrogels formed at lower pH are very rigid and so unable to withstand large deformations. This is similar to that reported for other related systems.[10] The data for the gels prepared at lower GdL concentrations and hence higher final shows that the gels still have elastic gel-like structure until a strain of 8%, although the three-dimensional networks have already been broken under the strain of 1%.

To gain further insight linking the rheology to the local packing of the peptides, we prepared fibers from gels prepared using different amounts of GdL and hence different final pH. Comparison of the X-ray fiber diffraction patterns collected from "*in situ*" prepared fiber alignments indicates that all gels formed at all final pH values have the same underlying molecular architecture. The patterns obtained appear to exhibit reflections similar to those observed for the cross-β patterns observed from amyloid, showing a meridional reflection at 4.5 Å (Figure 12) corresponding to β-strand spacing along the fiber axis. The reflections observed are similar for the samples at different pH (also see Figure S2, Supporting Information). The patterns differ only in the extent

(42) Menger, F. M.; Caran, K. L. *J. Am. Chem. Soc.* **2000**, *122*, 11679–11691.

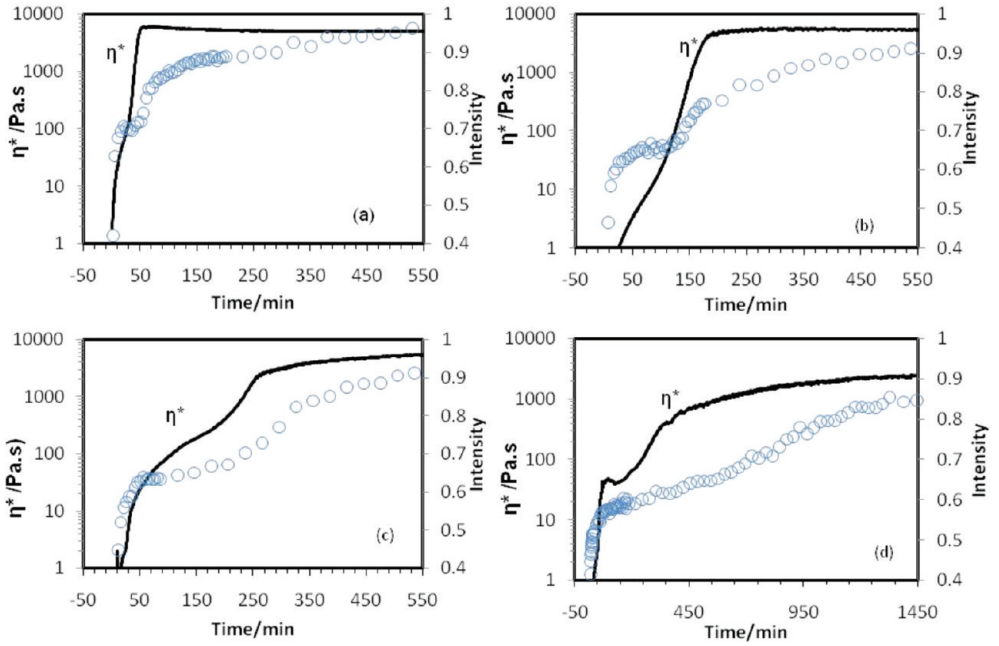

Figure 10. Relationship between complex viscosity η^* and fluoresence intensities for hydrogels prepared using different concentrations of GdL: (a) 14.42, (b) 5.96, (c) 4.46, and (d) 2.94 mg/mL.

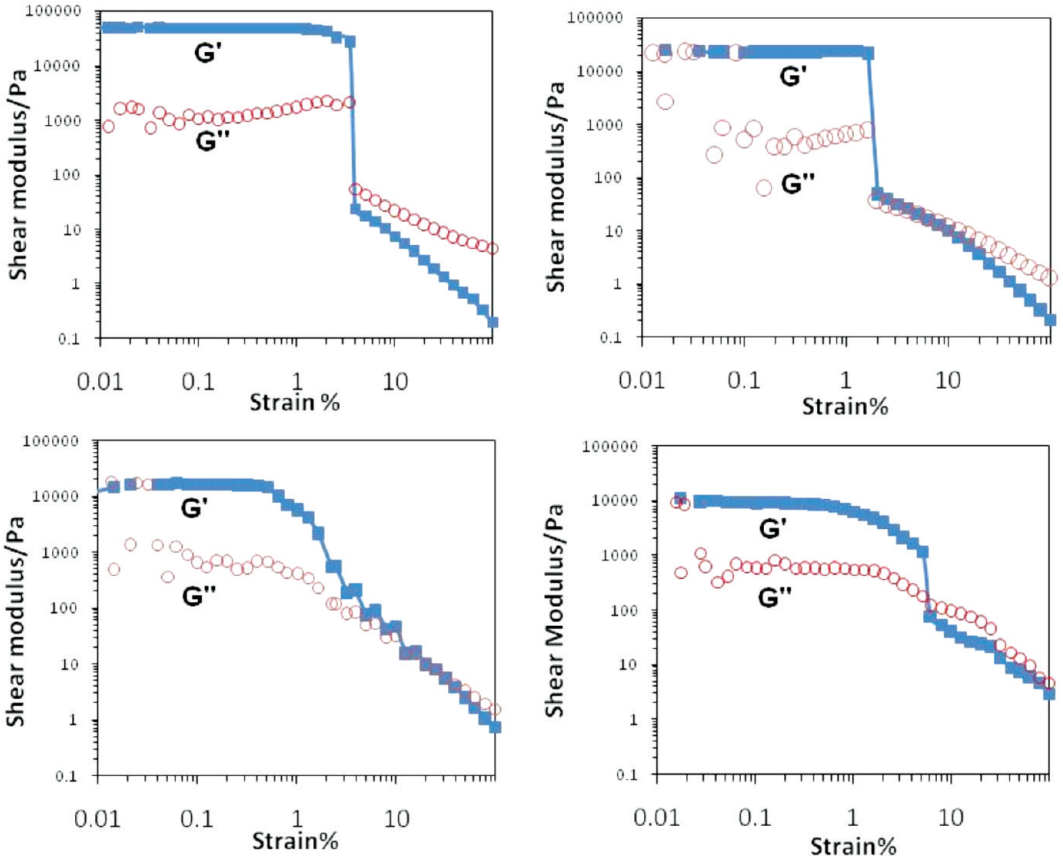

Figure 11. Strain sweeps for hydrogels prepared using different concentrations of GdL: (a) 14.42, (b) 5.96, (c) 4.46, and (d) 2.94 mg/mL. All data were collected at a frequency of 10 rad/s.

of alignment (shown by the degree of distinction between meridion and equator). In general, as pH is lowered orientation diminishes, as indicated by the major meridional reflections changing from well-defined arcs (pH 5.0) to rings (pH 3.1). These two observations are consistent with the behavior of the gels under strain as seen in the rheology measurements and the lateral association observed in the TEM. The data can describe a model whereby the molecular arrangement in the fibers is adopted rapidly at pH 5.0 (< 40 min), but the gel strength is low enough that these fibers can be aligned. As the pH continues to fall, the

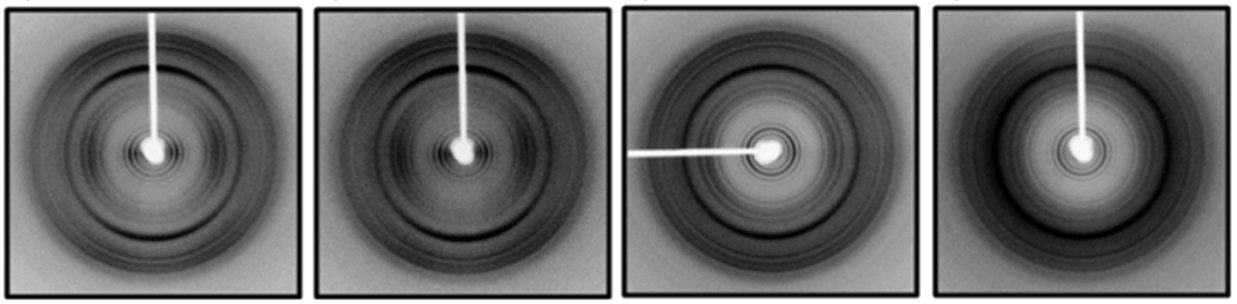

Figure 12. X-ray fiber diffraction patterns collected from "*in situ*" prepared fiber alignments from gels at a final pH from left to right of 5.0, 4.6, 3.6, and 3.1. All fiber axes are vertical to the diffraction patterns. The major meridional reflection is found to be at 4.5 Å and first major equatorial reflection found at 16 Å followed by a second grouping of reflections starting at 7.3 Å.

underlying molecular arrangement is unchanged but gel strength increases due to the increased lateral association of fibers.

Synchrotron fiber diffraction data showed the presence of two low-resolution equatorial reflections at 38 and 27 Å (data not shown). All the diffraction signal positions were examined using CLEARER, and a possible unit cell was determined.[31] Diffraction signals were indexed to the most likely unit cell (see Table S1, Supporting Information). The cell dimensions obtained were a = 37.90, b = 27.28, and c = 4.51 Å. The meridional 4.5 Å reflection is likely to arise from strand spacing along the fiber axis, as observed in amyloidogenic cross-β systems, and a similar strand spacing has been assigned in other dipeptide systems.[25] The equatorial reflections in the patterns arise from the unit cell dimensions perpendicular to the fiber axis and were used for unit cell determination.

We find that the unit cell may allow for more than one potential packing arrangement whereby naphthalene stacking is parallel to either the a or b axis. Many of the diffraction signals arise from higher order reflections from the unit cell itself (Table S1, Supporting Information), but the signals at 7.3 and 5.4 Å can be indexed as arising from a repetitive spacing within the unit cell, which we believe to result from naphthalene stacking, backed up by the CD data discussed above (Figure 3). We find it interesting to note that Smith et al. describe for the Fmoc−diphenylalanine system a β-strand spacing of 4.3 Å and a distance between pairs of aromatic fluorenyl groups of 7.6 Å,[25] very similar to what we observe here.

Conclusions

Combining all of these data, it is clear that the kinetics of self-assembly of the dipeptide derivative and hence hydrogelation is determined by the kinetics of pH adjustment. Using GdL, it is possible to adjust the kinetics of the pH drop, and hence we can probe the assembly process using a number of techniques. The importance of the kinetics of assembly has been described elsewhere for a temperature triggered assembly of aroyl L-cystine derivatives.[42] Similarly, the importance of history has been discussed for organogelators.[43] However, for the system described here, the assembly process requires a change in ionization state of the gelator. From the data, assembly begins as charge is removed from the C-terminus of the dipeptide derivative. The pK_a is higher than might be expected for the C-terminus of a dipeptide. However, this is in agreement with a recent report for Fmoc−diphenylalanine. IR shows that β-sheet assemblies are formed as the pH drops. The CD and LD data demonstrate that the assembly of the dipeptide derivative leads to a chiral organization of the naphthalene rings. This assembly occurs at relatively high pH (i.e., early on in the self-assembly process), with no increase in signal intensity after a pH of ∼4. From the fluorescence data with ThT, it is clear that the assembly occurs via a two-stage process—the first stage occurring at higher pH (∼5.2). This correlates well with the pK_a of the dipeptide derivative, indicating that the first stage of the assembly is associated with the removal of charge on the C-terminus of the dipeptide. This removal of charge allows lateral association of the dipeptides and hence β-sheet formation. Following this, a second stage of the assembly occurs, the kinetics of which are determined by the concentration of GdL added. This assembly leads to a matrix that has very similar rheological properties (as measured by G' and G''), indicating that this is not affected by the final pH. This is unsurprising—the only pH-sensitive group is the C-terminus, which will be fully protonated during this assembly. It may be that the kinetics of the assembly is driven by the kinetics of the primary assembly process, rather than the absolute pH. Indeed, it has been shown elsewhere for hydrogels prepared from a three-stranded β-sheet forming peptide that more rigid hydrogels are formed at higher temperatures (the trigger in this case).[44] Hence, faster kinetics of assembly leads to a more rigid gel. This was ascribed to either morphological differences in the fibrillar network (e.g., more physical cross-links) or alternatively intermolecular interactions that are dependent on the temperature of assembly. Similar effects may be occurring here. For the dipeptide studied here, the final mechanical properties of the hydrogels are very similar irrespective of the amount of GdL added; rather, the time to achieving the final gel is determined by the GdL concentration. The kinetics of the assembly has a clear effect on the ability of the networks to withstand strain, implying that it is the cross-links between fibers that are different, rather than the fibers themselves. This is confirmed from the X-ray fiber diffraction data. This data gives great insight into the assembly mechanism, demonstrating how assembly leads to hydrogelation.

Acknowledgment. We thank the EPSRC (EP/G012741/1) for funding.

Supporting Information Available: Further ThT fluorescence data at different GdL concentrations, one-dimensional graphical representation of the equatorial axes from X-ray fiber diffraction patterns, and comparison of the experimentally observed diffraction signals with the predicted signals from the determined unit cell. This material is available free of charge via the Internet at http://pubs.acs.org.

(43) Huang, X.; Raghavan, S. R.; Terech, P.; Weiss, R. G. *J. Am. Chem. Soc.* **2006**, *128*, 15341–15352.

(44) Rughani, R. V.; Salick, D. A.; Lamm, M. S.; Yucel, T.; Pochan, D. J.; Schneider, J. P. *Biomacromolecules* **2009**, *10*, 1295–1304.